Electronic supplementary information

A DNA aptamer for trivalent lanthanide ions with low nanomolar affinity

Jin Wang,[ab] Xin Wang,[bc] Xuesong Li,[bd] Xiangmei Li,[a] Hongtao Lei[a] and Juewen Liu*[b]

[a] Guangdong Provincial Key Laboratory of Food Quality and Safety, College of Food Science, South China Agricultural University, Guangzhou 510642, China;

[b] Department of Chemistry, Waterloo Institute for Nanotechnology, University of Waterloo, Waterloo, Ontario N2L 3G1, Canada;

[c] Beijing Laboratory for Food Quality and Safety, College of Food Science and Nutritional Engineering, China Agricultural University, Beijing 100083, China;

[d] School of the Environment and Safety Engineering, Jiangsu University, Zhenjiang 212013, China.

*Corresponding author Email: liujw@uwaterloo.ca

Chemicals

All DNA utilized were synthesized by Integrated DNA Technologies (Coralville, IA), with their respective sequences detailed in Table S1. Streptavidin-coated agarose resin possessed a loading capacity of 1-3 mg biotinylated BSA per milliliter was bought from Thermo Scientific (IL, USA). 6% BCL agarose bead standard (50-150 μM) was purchased from Agarose Bead Technologies (Spain). Scandium(III) chloride hydrate, yttrium(III) chloride hexahydrate, lanthanum(III) chloride hydrate, cerium(III) chloride hexahydrate, ammonium cerium(IV) nitrate, praseodymium(III) chloride hydrate, neodymium(III) chloride hydrate, samarium(III) chloride hydrate, europium(III) chloride hydrate, gadolinium(III) chloride hydrate, terbium(III) chloride hydrate, dysprosium(III) chloride hydrate, holmium(III) chloride hydrate, erbium(III) chloride hydrate, thulium(III) chloride hydrate, ytterbium(III) chloride hydrate, lutetium(III) chloride hydrate, calcium chloride, chromium(III) chloride hexahydrate, manganese(II) chloride hydrate, Iron(II) chloride tetrahydrate, iron(III) chloride hexahydrate, cobalt(II) chloride hexahydrate, nickel(II) chloride, copper(II) chloride dihydrate, zinc chloride, cadmium chloride hydrate, barium chloride dihydrate, mercury(II) acetate, lead(II) chloride and 2-mercaptoethanol were bought from Millipore-Sigma (Oakville, ON, Canada). The dNTP mix, Taq DNA polymerase with ThermoPol buffer, and a low-molecular-weight DNA ladder were obtained from New England Biolabs (Ipswich, MA). Micro Biospin chromatography columns and SsoFast EvaGreen supermix were procured from Bio-Rad Laboratories (Hercules, CA, USA). Thioflavin T (ThT), Amicon ultra-0.5 centrifugal filter unit (with 3K and 10K molecular weight cutoffs) were acquired from Millipore-Sigma (Oakville, ON, Canada). 2-(N-Morpholino) ethanesulfonic acid (MES) sodium salt, $MgCl_2 \cdot 6H_2O$, NaCl, $EDTA \cdot 2H_2O$, HCl and NaOH were obtained from Bio Basic Inc. (Toronto, ON, Canada). Milli-Q water (18.2 MΩ cm^{-1}) was used in all experiments.

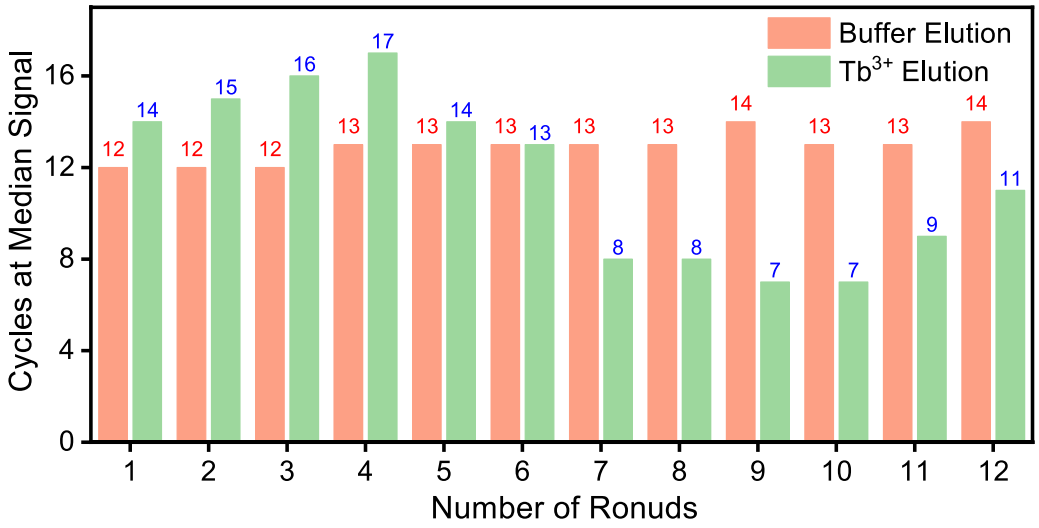

Figure S1. The real-time PCR results of the Tb^{3+} aptamer selection. Ideally, the green bars should be lower than the orange bars since we expect more DNA to be eluted by target metal ion than by the buffer. In the first five rounds, the opposite was observed and this was attributed to PCR inhibition by Tb^{3+}. In the later rounds, the released DNA became a lot more and the expected PCR cycle different was observed.

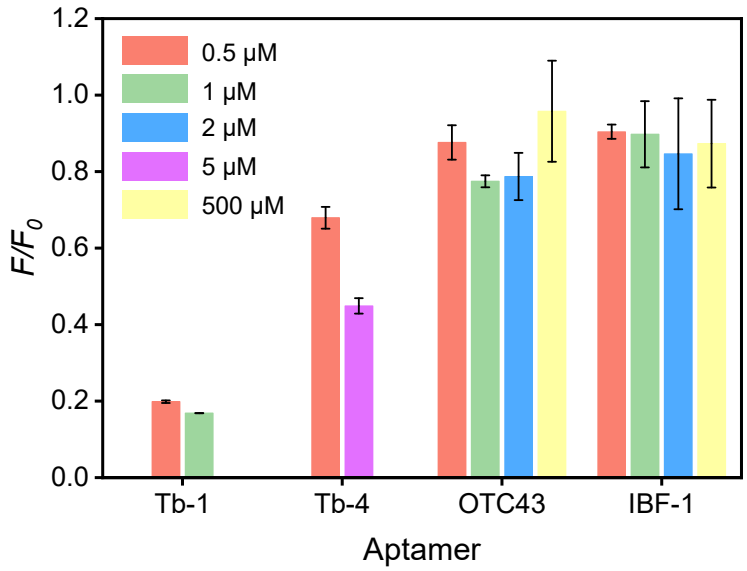

Figure S2. The response of different aptamers to various concentrations Tb^{3+} (aptamer: 0.5 μM, ThT: 1 μM) in 10 mM MES buffer (pH 6) with 100 mM NaCl and 2 mM $MgCl_2$. F_0 and F denote the fluorescence before and after adding Tb^{3+}, respectively. Without any metal added, the F/F_0 ratio is 1. A lower ratio indicates more fluorescence quenching attributable to metal binding.

Effect of salt for lanthanide binding

Most aptamer-target bindings depend on metal ions, particularly divalent metal ions.[1, 2] To investigate whether the binding of the Tb-1 aptamer requires metal ions, we employed the fluorescence assay to study the effects of Mg^{2+} and Na^{+} on Tb-1 binding. First, we fixed the Na^{+} concentration at 100 mM and varied the Mg^{2+} concentration at 0.1, 1, 5, 10, and 20 mM. The Mg^{2+} concentration of 1 mM showed the best fluorescence drop rate ($(F_0-F)/F_0$) (Figure S3A), so the Mg^{2+} concentration was ultimately set to 1 mM for further experiments. Then, we fixed Mg^{2+} concentration at 1 mM and varied Na^{+} concentration from 0 to 200 mM. At Na^{+} concentration of 10 mM, the fluorescence intensity and drop rate were relatively optimal, but overall, the buffers with varying concentrations of Na^{+} exhibited similar fluorescence drop rates (Figure S3B), suggesting that Na^{+} has no significant impact on the binding of Tb-1.

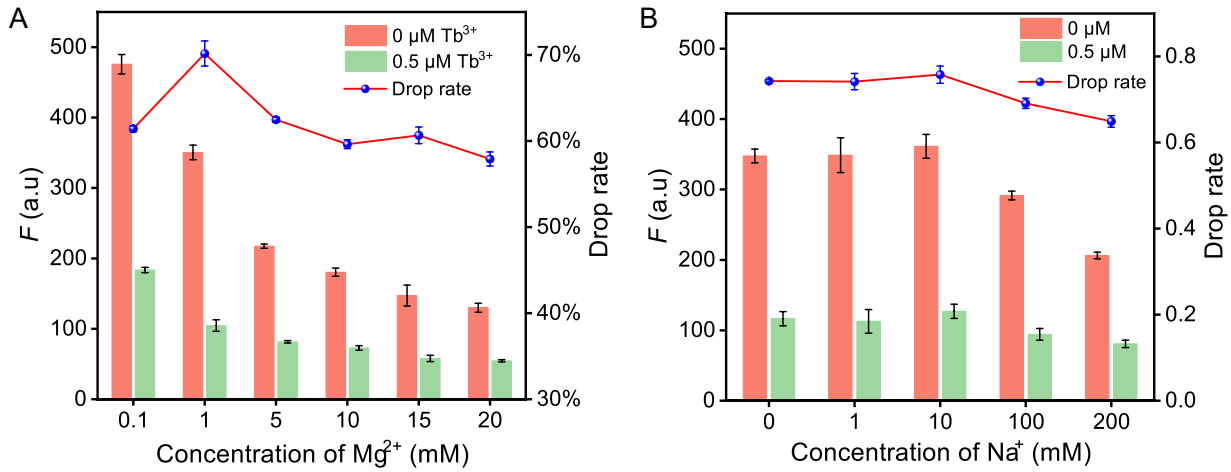

Figure S3. (A) The effect of Mg^{2+} concentration on Tb-1 binding in the presence of 100 mM Na^{+}. (B) The effect of Na^{+} concentration of Tb-1 binding in the presence of 1 mM Mg^{2+}. While higher salt concentration led to lower initial fluorescence, the relative fluorescence drop induced by Tb^{3+} did not change much.

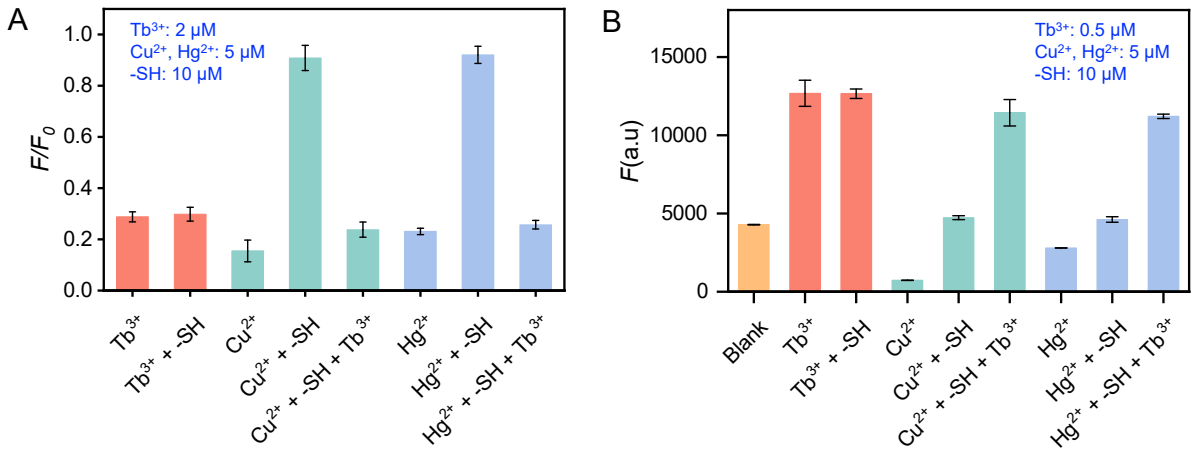

Figure S4. (A) Fluorescence response of different ions to the Tb-1/ThT mixture in 10 mM MES buffer (pH 6) with 100 mM NaCl and 2 mM $MgCl_2$ (Tb-1: 0.5 μM, ThT 1 μM). (B) Fluorescence changes upon adding different ions to 10 nM FAM Tb-1and 40 mM quencher labeled strand in 10 mM MES buffer (pH 6) with 100 mM NaCl and 2 mM $MgCl_2$. -SH means 2-mercaptoethanol.

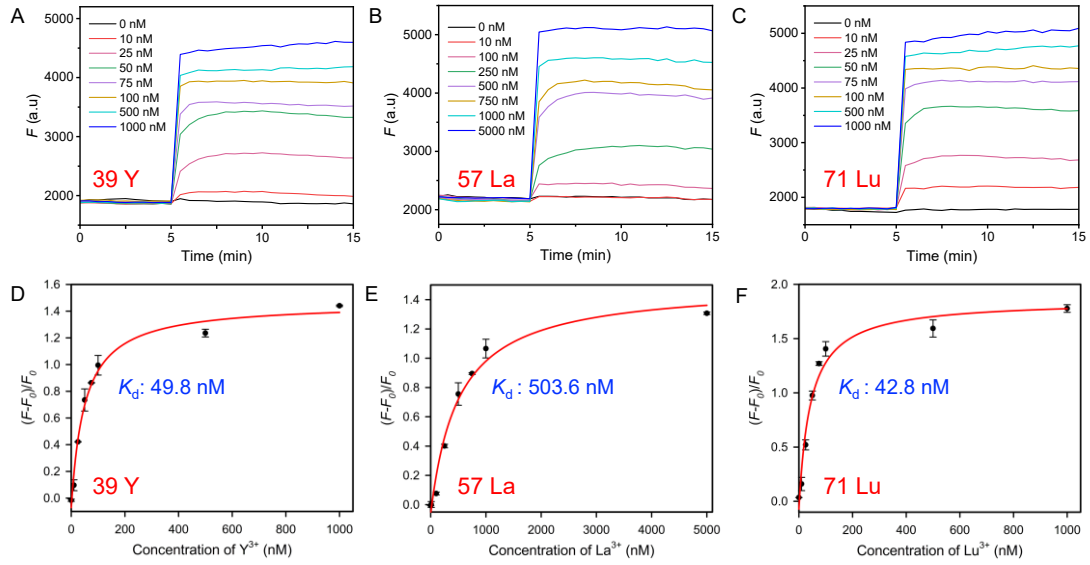

Figure S5. Kinetics traces of 20 nM FAM-based strand displacement biosensor in the presence of various concentrations of (A) Y^{3+}, (B) La^{3+}, and (C) Lu^{3+} in 10 mM MES buffer (pH 6) containing 100 mM NaCl and 2 mM $MgCl_2$. Note that lanthanide ions were added at the 5 min mark. Calibration curves of the biosensor for (D) Y^{3+}, (E) La^{3+}, and (F) Lu^{3+}.

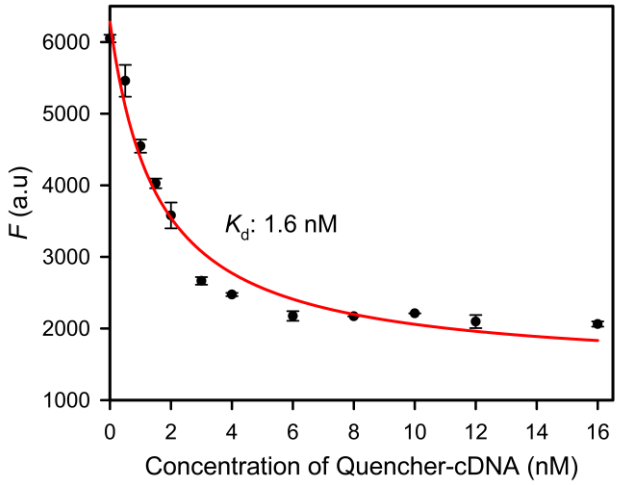

Figure S6. Fluorescence quenching of 5 nM of FAM Tb-1 with increasing concentrations of Quencher-cDNA in the SELEX buffer. This experiment allows us to obtain the K_d of the original aptamer based on Easley's work.[3]

The reaction of FAM Tb-1 (F) and Quencher-cDNA (Q) to form the FQ DNA complex as reaction 1, and the K_d for the reaction can be defined as $K_{d1} = \frac{[F][Q]}{[FQ]}$.

Similarly, the reaction FQ and Tb^{3+} to form F-Tb and Q as reaction 2, and the K_d for the reaction can be defined as $K_{d2} = \frac{[FQ][Tb]}{[F\text{-}Tb][Q]}$.

Therefore, the true K_d of reaction 3 (FAM Tb-1 and Tb to form F-Tb, the aptamer binding reaction) can be defined as $K_{d3} = K_{d1}\ K_{d2} = \frac{[F][Q]}{[FQ]}\ \frac{[FQ][Tb]}{[F\text{-}Tb][Q]} = \frac{[F][Tb]}{[F\text{-}Tb]}$.

Initially, we used 5 nM of FAM-labeled Tb-1 with increasing concentrations of Quencher-cDNA in the SELEX buffer. K_{d1} was directly fitted to be 2.8 nM (Figure S6). K_{d2} was using the apparent K_{d2} obtained from the calibration curve in Figure 3C. With 20 nM FAM Tb-1 and 40 nM Quencher-cDNA applied in the sensor, [Q] was 30 nM when Tb^{3+} matched the apparent K_d. Thus, $K_{d2} = \frac{[FQ][Tb]}{[F\text{-}Tb][Q]} = \frac{K_{d2\ apparent}}{[Q]}$ = 72.4 nM/30 nM = 2.41. Therefore, the true K_d, $K_{d3} = K_{d1}\ K_{d2}$ = 2.41 × 1.6 nM = 3.9 nM.

Similarly, the true K_d value for Y^{3+} is 2.7 nM, for La^{3+} is 26.9 nM, and for Lu^{3+} is 2.3 nM.

A **Ce Family 1**

Ce-1	GACGAC	CCGCG-CAGTGTAATTG--GTGAAAA--CAATTAC	GTCGTC	**89 reads**
Ce-7	GACGAC	CCGCGATAGTGTCTTGT--CCAATA--ACAAGAC	GTCGTC	**35 reads**
Ce-11	GACGAC	CCGCGTAAGTGTTTGAGG---CTTG---CTTCAAAC	GTCGTC	**28 reads**
Ce-12	GACGAC	CCGCG-TAGTGTTCTGAA---TGCAT--TTCAGAAC	GTCGTC	**26 reads**
Ce-14	GACGAC	CCGCGATAGTGCAGG---AATGTAAGTG---CCTGC	GTCGTC	**23 reads**
Ce-15	GACGAC	CCGCGCAAGTGTTTCAC--TTAGAT--GTGAAAC	GTCGTC	**20 reads**
Ce-16	GACGAC	CCGCGTAAGTAAACACC--TTTAAT--GGTGTTT	GTCGTC	**20 reads**
Ce-17	GACGAC	CCGCG--AGTATATCATACGAGTGCCGTAGGC----	GTCGTC	**20 reads**
Ce-20	GACGAC	CCGCGTAAGTGTAGTG--GCAATTGG--CACTAC	GTCGTC	**19 reads**

Ce Ungrouped Sequences

Ce-2	GACGAC	ACACAACTCGTGTTTTTTAAAGACTTGGGC	GTCGTC	**87 reads**
Ce-3	GACGAC	GAATCGAGGTAGTAAGTACTAGAAGACGA-	GTCGTC	**70 reads**
Ce-4	GACGAC	GGAAGTAGGGTACAAGGGCGGTAACTCTAG	GTCGTC	**56 reads**
Ce-5	GACGAC	GTGGGACGAAATCGCAGCATGAGACAGCAT	GTCGTC	**53 reads**
Ce-6	GACGAC	GCCGAGTGGAACGAAGGTGATCTGATCACA	GTCGTC	**46 reads**
Ce-8	GACGAC	AGCGAAGCCGAGTGATATCTACCACGAGTC	GTCGTC	**34 reads**
Ce-9	GACGCA	CTGCTGAAGGAATACATGGACGAACGTAGC	GTCGT-	**29 reads**
Ce-10	GACGAC	AGGTTGACTCAAGGATAGCGAGTACGACAT	GTCGTC	**29 reads**
Ce-13	GACGAC	GAGAAGCAAAACCGAAGTGTGACGGTTTAA	GTCGTC	**24 reads**
Ce-18	GACGAC	TGGCCCGCGTCTAGTATCTGAAAGATGCAA	GTCGTC	**20 reads**
Ce-19	GACGAC	CATGCGGAGCCTAACTCTCTCAGAGTTAGT	GTCGTC	**20 reads**

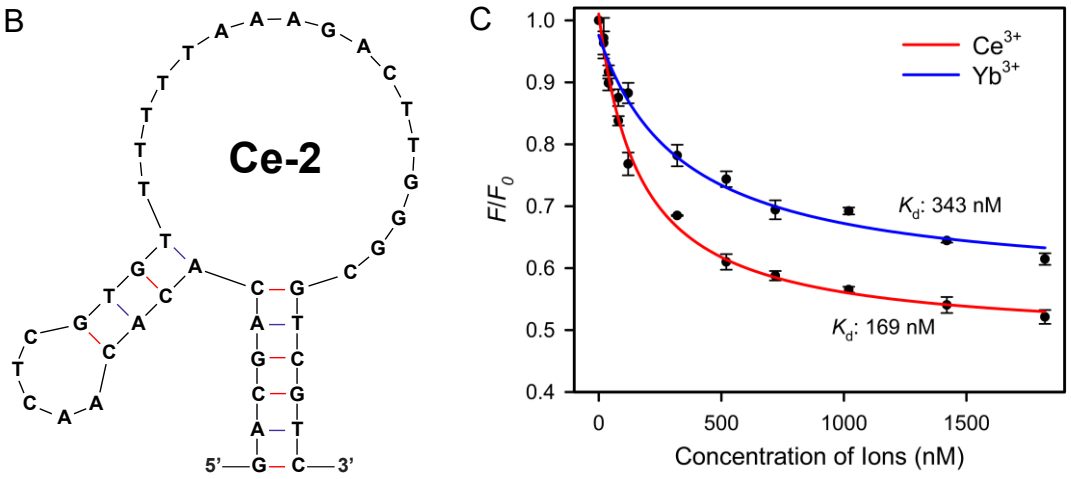

Figure S7. (A) Alignment of the top 20 sequences of Ce selection. Ce^{3+} selection Family 1 and Tb selection Family 1 belong to the same family. (B) The secondary structure predicted by mFold for the Ce-2 aptamer. (C) Binding of Ce^{3+} and Yb^{3+} to the Ce-2 aptamer.

Table S1. The DNA sequences used in this study.

DNA name	Sequences and modifications (5′ to 3′)
Library 1	GGAGGCTCTCGGGACGAC**N$_{30}$**GTCGTCCCGATGCTGCAATCGTAA
Library 2	GGAGGCTCTCGGGACGAC**N$_{30}$**GTCGTCCCGCCTTTAGGATTTACAG
Biotin-column	GTCGTCCCGAGAGCCATA**/3BioTEG/**
Forward primer	GGAGGCTCTCGGGACGAC
Reverse primer	TTACGATTGCAGCATCGGGACG
Biotin-reverse primer	**/5Biosg/**TTACGATTGCAGCATCGGGACG
P5-501	AATGATACGGCGACCACCGAGATCTACACTAGATCGCACACTCTTTCCCTACACGACGCTCTTCCGATCTTTACGATTGCAGCATCGGGACG
P5-502	AATGATACGGCGACCACCGAGATCTACACCTCTCTATACACTCTTTCCCTACACGACGCTCTTCCGATCTTTACGATTGCAGCATCGGGACG
P7-701	CAAGCAGAAGACGGCATACGAGATTCGCCTTAGTGACTGGAGTTCAGACGTGTGCTCTTCCGATCTGGAGGCTCTCGGGACGAC
P7-702	CAAGCAGAAGACGGCATACGAGATCTAGTACGGTGACTGGAGTTCAGACGTGTGCTCTTCCGATCTGGAGGCTCTCGGGACGAC
FAM-Tb-1	**/56-FAM/**CTCTCGACGACGGGGTAGAGGGTACGTAGTAATCCGGGTTAGTCGTC
Quencher-cDNA	AGTCGTCGAGAG**/3IABkFQ/**
Tb-1a	GACGACGGGGTAGAGGGTACGTAGTACCCGGGTTAGTCGTC
Tb-1b	GACGACGGGGTAGAGGGTACGTAGTAATCCGTTGGAGTCGTC
Gd-1	CTCGGGACGACCAGTTGGTCCCGCTTTATGTGTCCCGAG
OTC43	GAGGACTGGACCCTTCTCTGGTAGATTCTATCTAATGTCGTC
IBF-1	GACGACCAAAGGTAGCTTACGGTGGACCTGGGTTTGGTCGTC
Sc-1	GACGACGGACCATTCCCGTGGAATGACTACGTATATGTCGTC

Note: /3BioTEG/ is biotinylation at the 3′-end with extended spacer and /5Biosg/ is biotinylation at the 5′-end.

References

1. F. Yutong Huang, P. Kumar Lat and D. Sen, Unusual Paradigm for DNA–DNA Recognition and Binding:“Socket-Plug” Complementarity, *J. Am. Chem. Soc.*, 2023, **145**, 3146-3157.
2. Y. Liu and J. Liu, Selection of DNA aptamers for sensing uric acid in simulated tears, *Analysis & Sensing*, 2022, **2**, e202200010.
3. J. Hu and C. J. Easley, A simple and rapid approach for measurement of dissociation constants of DNA aptamers against proteins and small molecules via automated microchip electrophoresis, *Analyst*, 2011, **136**, 3461-3468.